

## Grain growth and mechanical properties of CeO<sub>2-x</sub> films deposited on glass substrates by closed field unbalanced magnetron sputtering technique

L. S. Chuah<sup>a,\*</sup>, H. Bilal<sup>a</sup>, Z. T.T. Jiang<sup>b</sup>

<sup>a</sup> *Department of Physics, School of Distance Education, Universiti Sains Malaysia, 11800 Minden, Penang, Malaysia.*

<sup>b</sup> *Surface Analysis and Materials Research Group, School of Engineering & Information Technology, Murdoch University, Murdoch, Western Australia 6150, Australia*

CeO<sub>2</sub> films with five different oxygen flow ratios, namely 1179°C, 1180°C, 1181°C, 1182°C, 1183°C and 1184°C were synthesized on glass substrates via closed field unbalanced magnetron sputtering technique. These films were characterized using many techniques such as X-ray diffraction (XRD), Field Emission Scanning Electron Microscope (FE-SEM), and UV-Vis-NIR. When the post-annealing temperature (TPA) for the films was increased from 1179°C to 1183 °C, a reduction of oxygen in the film was observed, which led to a phase transition from cubic to hexagonal Ce<sub>2</sub>O<sub>3</sub> (002). The phase transition is related to Ce<sub>4</sub> to Ce<sub>3</sub> transformation due to the formation of oxygen vacancies. XRD studies revealed that all samples have a cubic fluorite CeO<sub>2</sub> structure (space group: Fm3m) with a preferred orientation along (1 1 1) except for 1179 °C and 1181°C which prefer (2 2 0) plane orientation. Sample 1179°C showed the highest roughness (3.72nm) while sample 1184 °C has the lowest roughness (1.72nm). Sample 1181 °C showed highest percentage transmittance (>50%) while the other samples showed a percentage transmittance lower than 50%. Most of the films obtained exhibits a smooth and crack free surfaces.

(Received November 7, 2024; Accepted January 3, 2025)

*Keywords: CeO<sub>2</sub>; sputtering; XRD; FESEM*

### 1. Introduction

Cerium is the most abundant rare earth elements and it is made up about 0.0046 wt % of the Earth's crust (Rare Earth Elements Critical Resources for High Technology, 2002) [1]. In general, cerium can exist in two oxidation states: Ce<sup>3+</sup> and Ce<sup>4+</sup>. Therefore, cerium oxide or ceria can have two different oxide forms, CeO<sub>2</sub> (Ce<sup>4+</sup>) or Ce<sub>2</sub>O<sub>3</sub> (Ce<sup>3+</sup>), in bulk material. In recent years, the rare earth family has been applied extensively in many fields because of their unique physical and chemical properties which are significantly different from those of bulk materials (Masui, Fujiwara, Machida, & Adachi, 1997)[2].

The CeO<sub>2</sub> nanoparticles can be synthesized by using several methods such as solution precipitation (Chen & Chang, 2005) [3], sonochemical (Yu, Zhang, & Lin, 2003) [4], hydrothermal (Yan et al., 2012a) [5], solvothermal (Sun, Li, Zhang, & Wang, 2005) [6], ball milling (Yadav & Srivastava, 2012) [7], thermal decomposition (Wang, Mori, Li, & Ikegami, 2002) [8], thermal hydrolysis (Hirano, Fukuda, Iwata, Hotta, & Inagaki, 2000) [9] and sol-gel methods (Darroudi, Sarani, Kazemi, Khorsand, et al., 2014) [10]. These have been successfully used to create ceria nanoparticles and thin films (Lu, Turkovi, Dub, & Bernstorff, 2007) [11]. In recent years, researchers show great interest on ceria or cerium oxide nanoparticle film due to its interesting physical and chemical properties. These thin films can be coated on substrates by using several techniques such as magnetron sputtering, electron beam evaporation, metal organic chemical vapour deposition, flash evaporation, spray pyrolysis, and sol-gel method. Among these deposition techniques, magnetron sputtering technique is proven to be the best technique to prepare solid electrolyte materials and has been utilized in semiconductor industry. Cerium oxide has outstanding physical

---

\* Corresponding author: chuahleesiang@usm.my

<https://doi.org/10.15251/JOBM.2025.171.1>

and chemical properties, therefore it is used in various areas such as gas sensors, fuel cells, solar cells, catalysts, buffer layers with silicon wafer, UV absorbents and filter, hydrogen storage materials (Sohlberg, Pantelides, & Pennycook, 2008), electrochemistry and as a coating material.

## 2. Experimental

CeO<sub>2</sub> thin film was deposited on a glass substrate using TEER UDP450/4 closed field unbalanced magnetron sputtering ion plating system (Teer Coatings LTD, UK). The background pressure prior to coating and working gas pressure during sputtering were maintained at  $4 \times 10^{-5}$  Pa and 0.3 Pa, respectively. The deposition was performed under room temperature without external heating. The flow rate of argon gas (Ar, 99.999 %) and oxygen gas (O<sub>2</sub>, 99.999%) were controlled by MKS mass flow controllers. The deposition time of CeO<sub>2</sub> coating was varied to maintain the thickness of the deposition. The sample preparation conditions are shown in Table 1.

Table 1. Sample preparation conditions.

Sample	Oxygen flow ratio (%)	Gas flow (sccm)	Deposition rate (nm/min)	Deposition time (sec)
1179C	0	Ar/O <sub>2</sub> = 35/0	38.3	313
1180C	7	Ar/O <sub>2</sub> = 32.5/2.5	9.0	1333
1181C	14	Ar/O <sub>2</sub> = 30/5	11.0	1090
1182C	28	Ar/O <sub>2</sub> = 25/10	15.5	774
1183C	42	Ar/O <sub>2</sub> = 20/15	17.6	682
1184C	56	Ar/O <sub>2</sub> = 15/20	17.3	694

The samples were characterized by using several characterization techniques such as X-ray Diffraction (XRD), atomic force spectroscopy (AFM), Raman Spectroscopy (Jobin Yvon HR800 UV), Field Emission Scanning Electron Microscope (FESEM) and UV-VIS-NIR spectrometry. XRD patterns of the samples were investigated by an X'Pert PRO MRD analytical diffractometer (PW-3040/60 Netherlands) with Cu K $\alpha$  radiation ( $\lambda = 1.5418 \text{ \AA}$ ) at 40 kV and 40 mA in the range of 20° to 90° in order to determine the crystalline phase present in the sample. FESEM images of samples were studied using a LEO SUPRA 50 VP (Carl-Ziess SMT, Oberkochen, Germany). The samples were mounted on a specimen stub by using a double-sided tape. The surface morphology of the samples was investigated by choosing different magnifications. The optical properties of the samples were studied using a UV-VIS-NIR Spectrometer (Cary 5000, Agilent Technologies, USA). In the wavelength range of 200 to 900nm.

## 3. Result and discussion

Figure 1 shows the XRD patterns of the magnetron sputtered CeO<sub>2</sub> thin films grown at different substrate conditions. The XRD pattern of CeO<sub>2</sub> (sample: 1183 °C and 1184°C) has two distinct peaks observed at  $2\theta$  values of 28° and 47° corresponding to the crystal planes of (1 1 1) and (2 2 0) respectively. These values correspond to a cubic fluorite CeO<sub>2</sub> structure (space group: Fm3m; JCPDS No. 81-0792) with a strong preferred orientation along (1 1 1) plane. The XRD pattern of CeO<sub>2</sub> (sample: 1179 °C and 1181 °C) also has two distinct peaks observed at  $2\theta$  values of 28° and 47° which corresponds to the crystal planes of (1 1 1) and (2 2 0), respectively.

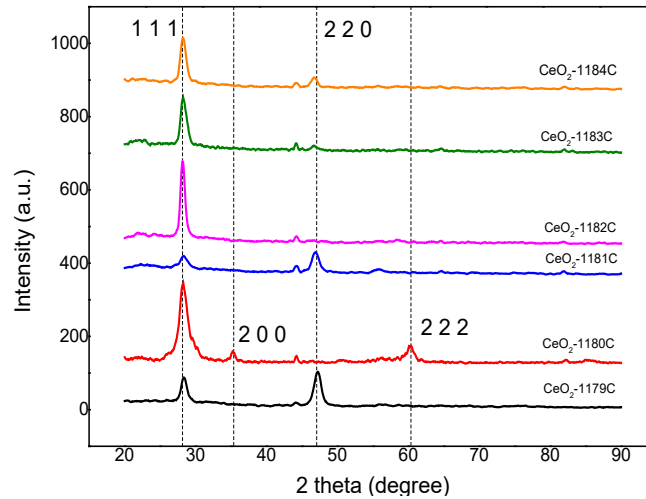


Fig. 1. XRD patterns of magnetron sputtered CeO<sub>2</sub> grown at different substrate conditions.

However, the intensity of the peaks for the plane (2 2 0) is more dominant compared to the plane (1 1 1) and these values corresponds to cubic fluorite CeO<sub>2</sub> structure (space group: Fm3m; JCPDS No. 34-0394) with a strong preferred orientation along (2 2 0) plane. It was observed that, the intensity of peak at 2θ values of 47° in sample 1180 °C and 1182 °C were diminished and the peak intensity at the plane (1 1 1) is highest among all samples. By using these conditions, CeO<sub>2</sub> with an orientation along the plane (1 1 1) was successfully formed. Two extra peaks at 2θ values of 35° and 60° were formed for sample 1180 °C. These peaks correspond to the crystal planes of (2 0 0) and (2 2 2), respectively.

The crystallite size (*d*), lattice parameter (*a*), dislocation density ( $\delta$ ) and strain ( $\epsilon$ ) are calculated by using the relations

$$d = \frac{0.9\lambda}{B\cos\theta}$$

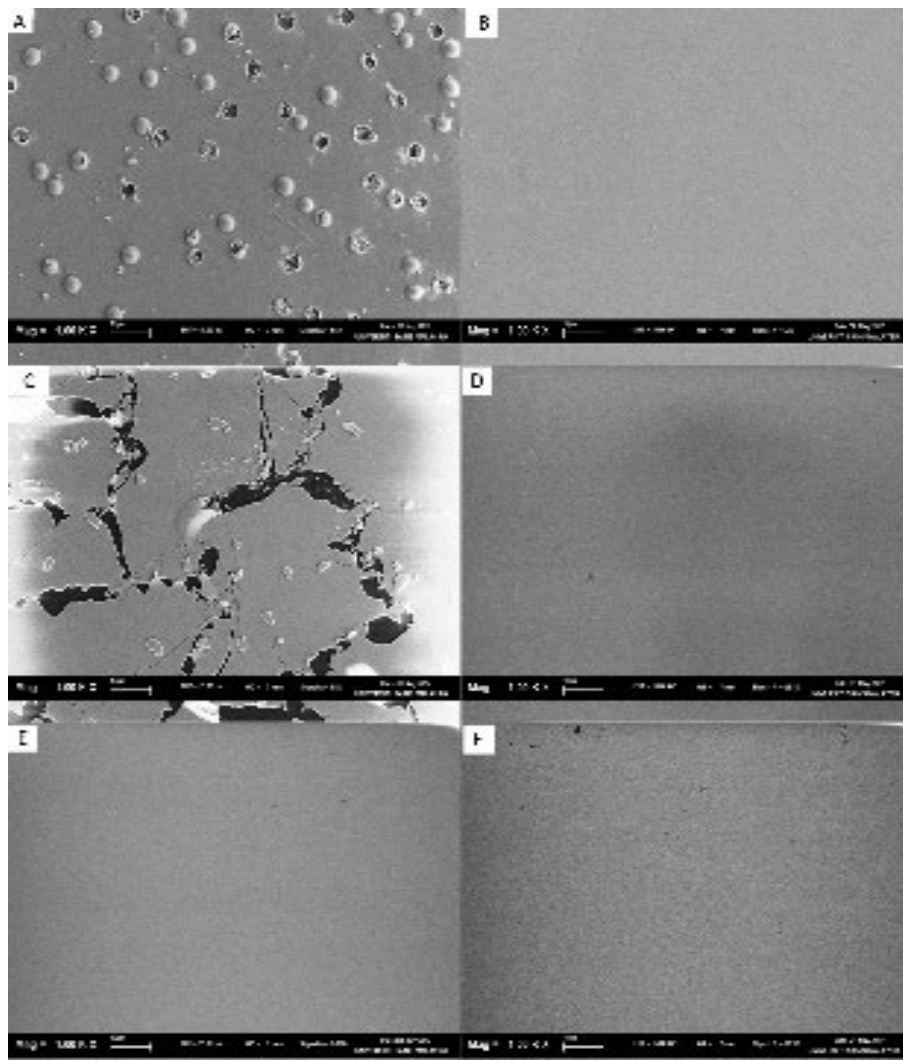
where  $\lambda$ ,  $\theta$ , *hkl* and *B* are the X-ray wavelength (1.54 Å), Bragg diffraction angle, miller indices and line width at half-maximum (FWHM), respectively. Micro structural parameters such as dislocation density, micro strain and number of crystallites per unit area are calculated and are tabulated in Table 2.

Table 2. Micro structural parameters of the samples.

Sample	crystallite size, <i>d</i> (nm)	lattice parameter, <i>a</i> (Å)	dislocation density ( $\delta$ ) ( $\times 10^{16}$ ) lines/m <sub>2</sub>	strain ( $\epsilon$ ) ( $\times 10^{-3}$ )
1179°C	8.42	5.92692	1.410509	14.10508855
1180°C	5.85	5.65099	2.922054	29.22054204
1181°C	9.73	5.96996	1.056268	10.56268478
1182°C	13.00	5.64262	0.591716	5.917159763
1183°C	8.81	5.63309	1.288392	12.88392486
1184°C	10.64	5.65099	0.883317	8.833173158

SEM images of CeO<sub>2</sub> samples at 1 kx and 10 kx magnification are shown Figure 2 and Figure 3. Scanning electron microscopy is proved to be a convenient and versatile method to analyze surface morphology of thin films. From Figure 2 and Figure 3, it is known that, the surface of the samples 1179 °C and 1181 °C are not uniform compared to the surface of the samples 1180 °C, 1182 °C, 1183 °C and 1184 °C. SEM image of sample 1179 °C (image A) indicates the formation of bubble-like structure on the surface of the film. Some of the bubbles are distorted and broken while

some remain intact. As for the sample 1181C (image C), several cracks are observed on the surface of the film, while the other remaining sample shows an even and uniform surface. Images that taken at higher magnification (Figure 3) reveals that all samples have rough surface.



*Fig. 2. SEM images of CeO<sub>2</sub> samples (a) 1179C, (b) 1180C, (c) 1181C, (d) 1182C, (e) 1183C, (f) 1184C at 1 kx magnification.*

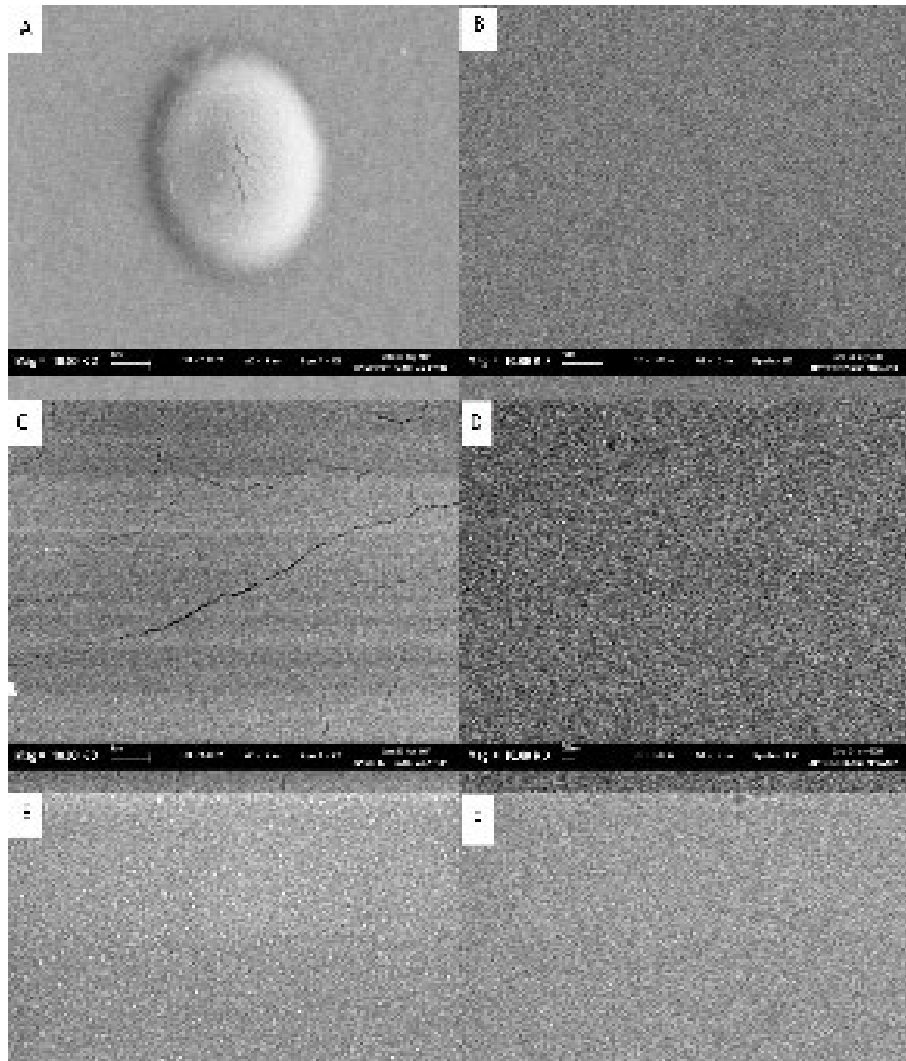


*Fig. 3. SEM images of CeO<sub>2</sub> samples (a) 1179C, (b) 1180C, (c) 1181C, (d) 1182C, (e) 1183C, (f) 1184C at 10 kx magnification.*

Figure 4 and 5 shows the absorption and transmission spectra of CeO<sub>2</sub> films deposited on glass substrate obtained from UV-VIS-NIR study. The prepared films are mainly transparent in the visible region and indicate that the films are uniform and well adhered to the glass substrates. An average transmittance greater than 50% were observed for the sample 1181°C, which was recorded as the highest percentage transmittance compared to the other samples. As for the sample 1180 °C, the percentage transmission is almost zero. This is due to the transparency of the film. In sample 1180 °C, the film coated on the glass substrate are found to be opaque.

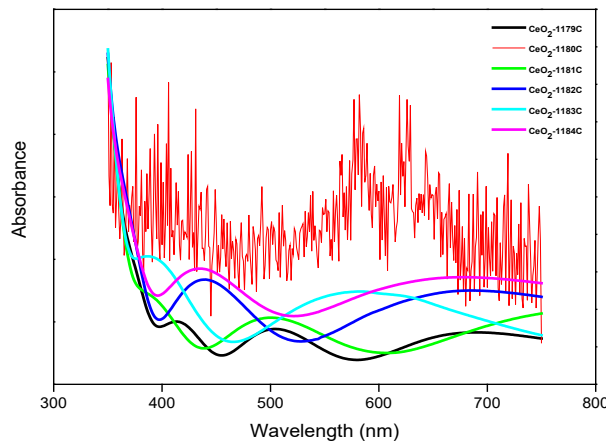


Fig. 4. Absorption spectra of magnetron sputtered  $\text{CeO}_2$  grown at different substrate conditions.

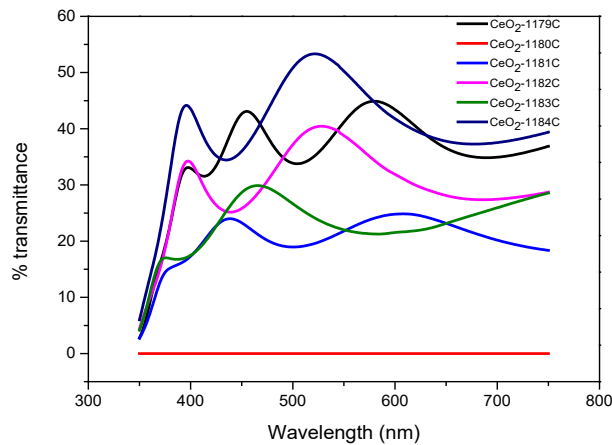


Fig. 5. Transmission spectra of magnetron sputtered  $\text{CeO}_2$  grown at different substrate conditions.

#### 4. Conclusion

Cerium oxide thin films have been successfully deposited on glass substrates using closed field unbalanced magnetron sputtering technique. All the films showed a crystalline and cubic fluorite structure with preferred orientation along (1 1 1) plane (samples: 1180 °C, 1182 °C, 1183 °C and 1184 °C) and (2 2 0) plane (samples: 1179 °C and 1180 °C). The formation of cubic fluorite structure from XRD analysis. The maximum crystallite size obtained was 13 nm (1182 °C). Most of the prepared films showed a crack free and smooth surface except for the sample 1179C and 1181C. The roughness of sample 1179 °C and 1181°C were among the highest compared to the other samples, which is 3.72nm and 3.14nm, respectively. All the films are transparent at visible region except sample 1184°C which has a percentage transmission reaching zero.

#### Acknowledgement

The support from Bridging Grant and Universiti Sains Malaysia is gratefully acknowledged.

## References

- [1] Rare Earth Elements Critical Resources for High Technology, 2002
- [2] T. Masui., K. Fujiwara., K. Machida, G. Adachi, (1997), Chemistry of Materials, 9, 2197-2204; <https://doi.org/10.1021/cm970359v>
- [3] H. Chen., H. Chang, (2005), ceramics international, 31, 795-802; <https://doi.org/10.1016/j.ceramint.2004.09.006>
- [4] J. Yu., L. Zhang., J. Lin, (2003), Colloid and Interface Science, 250, 240-243; [https://doi.org/10.1016/s0021-9797\(02\)00168-6](https://doi.org/10.1016/s0021-9797(02)00168-6)
- [5] Z. Yan., J. Wang., R. Zou., L. Liu., Z. Zhang., X. Wang, (2012) Energy Fuels, 26, 5879–5886; <https://doi.org/10.1021/ef301085w>
- [6] C. Sun., H. Li., H. Zhang., Z. Wang., L. Chen, (2005), Nanotechnology, 16, 1454-1463; <https://doi.org/10.1088/0957-4484/16/9/006>
- [7] T. P. Yadav., O. N. Srivastava, (2012) Ceramics International, 38, 5783-5789; <https://doi.org/10.1016/j.ceramint.2012.04.025>
- [8] Y. Wang., T. Mori., J. Li., T. Ikegami, (2002) Journal of The American Ceramic Society, 85, 3105-3107; <https://doi.org/10.1111/j.1151-2916.2002.tb00591.x>
- [9] M. Hirano., Y. Fukuda., H. Iwata., Y. Hotta., M. Inagaki, (2000), Journal of The American Ceramic Society, 85, 1287-1289; <https://doi.org/10.1111/j.1151-2916.2000.tb01371.x>
- [10] M. Darroudi., M. Sarani., R. K. Oskuee., A. K. Zak., H. A. Hosseini., L. Gholami, (2014) Ceramics International, 40, 2041-2045; <https://doi.org/10.1016/j.ceramint.2013.07.116>
- [11] M. I. lavčević., A turković., P. dubček., S. bernstorff, (2007) thin solid films, 515, 5624-5626; <https://doi.org/10.1016/j.tsf.2006.12.014>